

Precoding with Received-Interference Power Control for Multibeam Satellite Communication Systems

Eva Lagunas^{1,*}, Ana Pérez-Neira^{2,3}, Marc Martínez³, Miguel Angel Lagunas^{2,3}, Miguel Angel Vázquez² and Björn Ottersten¹

¹ SnT, University of Luxembourg, Luxembourg

² Centre Tecnologic de les Telecomunicacions de Catalunya (CTTC/CERCA), Castelldefels, Spain

³ Universitat Politècnica de Catalunya (UPC), Barcelona, Spain

Correspondence*:

Dr. Eva Lagunas, 29 Av. JF Kennedy L-1855 Luxembourg Ville (Luxembourg)
eva.lagunas@uni.lu

2 ABSTRACT

3 Zero-Forcing (ZF) and Regularized Zero-Forcing (RZF) precoding are low-complexity sub-
4 optimal solutions widely accepted in the satellite communications community to mitigate the
5 resulting co-channel interference caused by aggressive frequency reuse. However, both are
6 sensitive to the conditioning of the channel matrix, which can greatly reduce the achievable gains.
7 This paper brings the attention to the benefits of a design that allows some residual received
8 interference power at the co-channel users. The motivation behind this approach is to relax the
9 dependence on the matrix inversion procedure involved in conventional precoding schemes. In
10 particular, the proposed scheme aims to be less sensitive to the user scheduling, which is one of
11 the key limiting factors for the practical implementation of precoding. Furthermore, the proposed
12 technique can also cope with more users than satellite beams. In fact, the proposed precoder
13 can be tuned to control the interference towards the co-channel beams, which is a desirable
14 feature that is not met by the existing RZF solutions. The design is formulated as a non-convex
15 optimization and we study various algorithms in order to obtain a practical solution. Supporting
16 results based on numerical simulations show that the proposed precoding implementations are
17 able to outperform the conventional ZF and RZF schemes.

18 **Keywords:** Satellite Communications, Precoding, Zero-Forcing, Received-Interference Power Control, User scheduling

1 INTRODUCTION

19 The satellite communication industry is witnessing a revolution, motivated by the unprecedented global
20 demand for broadband data services (Kodheli et al., 2020). Recent developments on space technology have
21 already achieved more throughput and lower cost per bit making use of multiple narrowly focused spot
22 beams, which enable tighter frequency reuse. As the broadband connectivity demand is likely to continue
23 growing at a rapid pace, the future of the space sector relies on the development of Ultra High Throughput

24 Satellite (UHTS) systems, combined with flexibility to seamlessly deliver cost-competitive connectivity in
25 response to evolving consumer demand and price expectations.

26 For UHTS to become a reality, more aggressive frequency reuse is essential in order to achieve higher
27 spectral efficiency and much lower cost per bit. The reuse of spectrum automatically translates into
28 cochannel interference, which can be mitigated via precoding (Vázquez et al., 2016; Perez-Neira et al.,
29 2019), assuming that the interference channel coefficients are properly estimated at each user terminal
30 and reported back to the satellite gateway. In satellite communications, precoding refers to the waveform
31 design (i.e. involving the transmitted symbols) and is applied on-ground in the satellite gateway. This is
32 different from *beamforming*, which refers to the beam pattern shaping and is applied on-board the satellite.
33 For example, multi-antenna architectures with beam-forming capabilities have been recently considered in
34 satellite communications (Cailloce et al., 2000). In this paper, we assume that the beamforming is given
35 under a multi-feed-per-beam architecture, meaning that multiple antenna elements are used to conform a
36 single beam, which is linked to a single Radio Frequency (RF) chain (Toso et al., 2014).

37 Precoding is typically applied over a predefined beam pattern, as certain level of cochannel interference
38 results from the beam sidelobes leakage. Precoding benefits for interference mitigation in multibeam
39 satellite systems have been widely studied in the literature, e.g. (Vázquez et al., 2018; Zheng et al., 2012;
40 Christopoulos et al., 2015; Taricco, 2014). Theoretical studies carried out at the European Space Agency
41 (ESA) showed that important rate gains (beyond 40%) can be achieved with the application of precoding
42 (Arapoglou et al., 2016). ESA is also currently carrying out the first over-the-satellite precoding test for a
43 simplified 2-beam system (ESA project LiveSatPreDem, 2020).

44 The most popular low-complexity precoding design in satellite communications is the Regularized
45 Zero-Forcing (RZF) precoding (Zetterberg and Ottersten, 1995; Peel et al., 2005) (sometimes referred to as
46 MMSE precoding). The key idea behind RZF is to introduce a regularized form of inversion that improves
47 performance, particularly for very low channel coefficients which otherwise incur an unavoidable power
48 consumption. Matrix regularization is a common tool to achieve numerical stability and robustness to the
49 inverse computation of ill-conditioned matrices (Bjornson et al., Jul. 2014).

50 The regularization factor of the RZF precoding has no close solution and depends on the criteria of
51 the engineer. One possible metric for choosing it is to maximize the Signal-to-Interference and Noise
52 Ratio (SINR) as suggested in (Peel et al., 2005; Bengtsson and Ottersten, 1999; Bjornson et al., Jul. 2014),
53 but a closed-form optimal regularizer only exists under some specific assumptions: the number of users
54 is not larger than then number of satellite beams, homogeneous SINR conditions, and in some of the
55 developments, such as (Peel et al., 2005), in the limit of large number of users. Still, the regularizer
56 proposed in (Peel et al., 2005; Bengtsson and Ottersten, 1999; Bjornson et al., Jul. 2014) is the most
57 commonly used in the satellite communications literature (Devillers et al., 2011; Taricco, 2014; Lagunas
58 et al., 2018; Perez-Neira et al., 2019; Vázquez et al., 2018).

59 Precoding in the satellite communications context is characterized by a large number of users compared
60 with the number of beams. Therefore, appropriate techniques to cope with this situation are mandatory,
61 either by appropriately managing the available degrees of freedom and/or by performing the right user
62 scheduling. These techniques have an important impact on the final precoding performance (Lagunas et al.,
63 2018; Bandi et al., 2020). For instance, depending on the scheduled users, the corresponding channel
64 matrix may result more or less tractable depending on the orthogonality of the different channel vectors
65 (Taesang Yoo and Goldsmith, 2006). If the orthogonality of the scheduled users' channel vectors is low, the

performance of the RZF precoding will suffer (as we demonstrate in the results section). This is because the resulting channel matrix, even if heuristically regularized, is difficult to perform.

This paper brings the attention to the benefits and practicality of a precoding design that allows some residual received interference power at the cochannel users. The motivation behind this approach is to relax the dependence on the matrix inversion procedure involved in conventional satellite precoding schemes. In particular, we list below the contributions of this paper:

- We formulate the precoding problem as a maximization of the transmit power towards the desired beam while imposing a number of received interference power constraint towards the co-channel beams, and keeping the total transmit power under certain limit. The resulting optimization problem with received interference power constraints appears to be non-convex in its direct form.
- Subsequently, we show that the non-convexity can be addressed under different alternatives: a Semidefinite Programming (SDP) (inspired by (Luo et al., 2010)), a Second-Order Cone Programming (SOCP) formulation (see (Vorobyov et al., 2003; Gershman et al., 2010)), and a new relaxation proposed by the authors in (Lagunas et al., May 2020). The relaxed solution is shown to have a closed-form expression with a similar structure as the RZF but with the regularization factor being a function of the tolerable interference at the receiver side. Furthermore, the relaxed proposed solution does not require that the number of users is equal or smaller than the number of beams.
- We compare the different solutions in terms of optimality and computational complexity, and we test them versus the conventional ZF and RZF. Substantial rate gains are achievable even when random user scheduling is considered, confirming that the proposed solution is less sensitive to the user scheduling.

The rest of this paper is organized as follows. Section 2 introduces the GEO multibeam satellite system model. Section 3 presents the precoding benchmarks considered in this paper. Section 4 introduces the proposed precoding scheme, its optimization framework and the proposed solutions. Supporting simulation results are presented in Section 5, and finally, concluding remarks are provided in Section 6.

2 SYSTEM MODEL

Consider the forward link of a bent-pipe GEO multi-beam satellite system with N beams. User terminals are assumed to be randomly distributed over the coverage area. In general, we assume that a single user terminal is served per beam during a specific time slot. In addition, we consider an ideal feeder link between gateway and satellite. The impact of imperfect CSI is out of the scope of this work. The reader is referred to (Arapoglou et al., 2016) for the impact of channel estimation errors and outdated CSI for the satellite standard DVB-S2(X). The considered system is illustrated in Fig. 1.

All beams re-use the same frequency band B . Linear precoding is implemented to mitigate the resulting co-beam interference, assuming perfect Channel State Information (CSI) at the satellite gateway. Let u_n be the information symbol intended to the user located in the n -th beam, which satisfies the unit average energy condition $\mathbb{E}[|u_n|^2] = 1$. The precoded symbols $\mathbf{x} = [x_1 \ \cdots \ x_N]^T$, with x_n being the symbol transmitted over the n -th beam, can be expressed as,

$$\mathbf{x} = \sum_{n=1}^N \mathbf{w}_n u_n, \quad (1)$$

where \mathbf{w}_n denotes the $N \times 1$ precoding vector for the user located in the n -th beam, and the total transmit power satisfies $\sum_{n=1}^N \|\mathbf{w}_n\|^2 \leq P_{\text{tot}}$. The digital base band model for the observed signal at the user located

103 in the n -th beam can be written as,

$$\begin{aligned} y_n &= \mathbf{h}_n^H \mathbf{x} + n_n \\ &= \mathbf{h}_n^H \mathbf{w}_n u_n + \mathbf{h}_n^H \sum_{m \neq n}^N \mathbf{w}_m u_m + n_n, \end{aligned} \quad (2)$$

104 where $\mathbf{h}_n \in \mathbb{C}^{N \times 1}$ is the channel vector from the satellite to the user located in the n -th beam, and the
 105 element n_n is a zero-mean unit-variance complex Gaussian noise. The precoding vectors can be rearranged
 106 in $\mathbf{W} = [\mathbf{w}_1 \ \mathbf{w}_2 \ \cdots \ \mathbf{w}_N]$, and the received signal vector can be expressed as $\mathbf{y} = \mathbf{H}\mathbf{x} + \mathbf{n}$, with
 107 $\mathbf{H} = [\mathbf{h}_1 \ \mathbf{h}_2 \ \cdots \ \mathbf{h}_N]^H$, $\mathbf{y} = [y_1 \ y_2 \ \cdots \ y_N]^T$ and $\mathbf{n} = [n_1 \ n_2 \ \cdots \ n_N]^T$.

108 The channel matrix \mathbf{H} accounts for the complex coefficients due to the considered beam pattern as well
 109 as for the link budget. In other words, $\mathbf{H} = \mathbf{L} \circ \mathbf{B}$, with matrix \mathbf{B} denoting the beam radiation pattern
 110 coefficients, \mathbf{L} denoting the link budget coefficients and the operator \circ denoting the Hadamard product.
 111 The link budget between the i -th user and the n -th beam is given by,

$$[\mathbf{L}]_{n,i} = \sqrt{\frac{G_R}{\eta K_B T_R B}} \left(4\pi \frac{d_n}{\lambda} \right)^{-1} \quad (3)$$

112 where G_R is the user terminal antenna gain, η is a coefficient modeling the on-board power losses and d_n
 113 is the slant range between the satellite and the k -th user. The term $\sqrt{K_B T_R B}$ represents the noise standard
 114 deviation, σ_n , where K_B is the Boltzmann constant and T_R is the receiver noise temperature. It is common
 115 practice to include the noise contribution into the channel model (Christopoulos et al., 2015; Joroughi et al.,
 116 Feb. 2017; Guidotti and Vanelli-Coralli, 2018) in order to proceed with the assumption of unit-variance
 117 noise. Note that $T_R = (NF - 1)T_0 + T$, where NF stands for the noise figure, $T_0 = 290^\circ K$ is the noise
 118 reference temperature and T is the noise temperature at the antenna dish.

119 According to (2), the SINR at the user located in the n -th beam can be expressed as,

$$\text{SINR}_n = \frac{|\mathbf{h}_n^H \mathbf{w}_n|^2}{\sum_{\substack{m=1 \\ m \neq n}}^N |\mathbf{h}_n^H \mathbf{w}_m|^2 + 1}. \quad (4)$$

120 Finally, and assuming Gaussian interference, the achievable rate in bps for the user located in the n -th
 121 beam is given by,

$$r_n = B \cdot \log_2 (1 + \text{SINR}_n). \quad (5)$$

3 CONVENTIONAL REGULARIZED ZERO-FORCING PRECODER

122 In this section, we briefly review the conventional regularized zero-forcing precoder normally used in the
 123 satellite communications literature (Devillers et al., 2011; Taricco, 2014; Lagunas et al., 2018; Vazquez
 124 et al., 2016; Vázquez et al., 2018).

125 First, let us introduce the general Zero-Forcing (ZF) motivation. Essentially, ZF “tries” to invert the
 126 channel coefficients. This is $\mathbf{h}_n^H \mathbf{w}_i = 0$, for $n \neq i$ (Bengtsson and Ottersten, 2001). However, although \mathbf{H}
 127 is a square $N \times N$ matrix, it may be rank-deficient and thus, not invertible. This may happen depending

on the location of the scheduled users. An alternative solution is the so-called pseudo-inverse, which is a specific generalized inverse. The pseudo-inverse is the baseline of the ZF precoder:

$$\mathbf{W}_{ZF} = \eta \mathbf{H}^H (\mathbf{H} \mathbf{H}^H)^{-1}, \quad (6)$$

with $\eta = \sqrt{P_{\text{tot}} / \text{Trace} \{ \mathbf{W}_{ZF} \mathbf{W}_{ZF}^H \}}$ being the normalization factor such that $\sum_{n=1}^N \|\mathbf{w}_n\|^2 = P_{\text{tot}}$.

Often the matrix $(\mathbf{H} \mathbf{H}^H)$ appears to be ill-conditioned, meaning with a condition number very large, rendering a close-to-singular matrix. In these cases, the computation of its inverse is prone to large numerical errors, resulting in significant performance loss due to the inaccuracy of the matrix inversion. To overcome this issue, the RZF was proposed in (Zetterberg and Ottersten, 1995), whose expression is given by,

$$\mathbf{W}_{RZF} = \eta' \mathbf{H}^H (\mathbf{H} \mathbf{H}^H + \alpha \mathbf{I})^{-1}, \quad (7)$$

where $\alpha > 0$ is the regularization factor, and $\eta' = \sqrt{P_{\text{tot}} / \text{Trace} \{ \mathbf{W}_{RZF} \mathbf{W}_{RZF}^H \}}$. By maximizing the SINR at the user terminals under the assumption of homogeneous SINR conditions, the optimal α can be set to N/P_{tot} if the noise has unit variance, (Peel et al., 2005) or, in other words, inversely proportional to the per-beam SINR (Bjornson et al., Jul. 2014). However, as highlighted in (Taesang Yoo and Goldsmith, 2006), the RZF design still suffers significant effective channel gain loss when \mathbf{H} is poorly conditioned.

4 REGULARIZED ZERO-FORCING PRECODER WITH RECEIVED-INTERFERENCE POWER CONSTRAINTS

Let us focus this section on the design of a particular precoding vector $\mathbf{w}_n, n = 1 \dots N$. The rest of the precoding vectors can be obtained in a similar manner.

The precoding vector associated to the user located in the n -th beam shall be designed to maximize the link gain towards that particular user, while satisfying received-power constraints towards the existing co-channel beams of the system. In other words, the design of each of the precoding vectors \mathbf{w}_n shall be given by the solution to the following quadratically constrained quadratic optimization problem (QCQP), where the objective corresponds to the nominator of (4) and the constraint (C1) limits the interference term in the denominator:

$$\begin{aligned} \max_{\{\mathbf{w}_n\}} \quad & \mathbf{w}_n^H \mathbf{R}_n \mathbf{w}_n \\ \text{s.t.} \quad & \mathbf{w}_n^H \mathbf{R}_m \mathbf{w}_n \leq P_m, \quad \text{for } m \neq n \quad (\text{C1}) \\ & \|\mathbf{w}_n\|^2 \leq P_{\text{max}}, \quad (\text{C2}) \end{aligned} \quad (8)$$

where $\mathbf{R}_n = \mathbf{h}_n \mathbf{h}_n^H$ and $\mathbf{R}_m = \mathbf{h}_m \mathbf{h}_m^H$ for $m \neq n$. Note that $\mathbf{w}_n^H \mathbf{R}_n \mathbf{w}_n$ is the received power at the user located in the n -th beam, and $\mathbf{w}_n^H \mathbf{R}_m \mathbf{w}_n, m \neq n$, is the power received by the users at the co-channel beams (i.e., users $m = 1 \dots N, m \neq n$). Clearly, the constraint (C1) denotes the received-power limits imposed to the co-channel beams, where P_m stands for the maximum interference power that is created by the n -th beam at a user in any of the other beams (i.e., m -th beam, $m \neq n$). Finally, the constraint (C2) restricts the total transmit power associated to the precoding vector \mathbf{w}_n to be below P_{max} , which can be fixed based on the total available power, e.g. $P_{\text{max}} = P_{\text{tot}}/N$.

156 The optimization problem in (8) is non-convex, because it is the maximization and not the minimization
 157 of a convex function within a convex set. In other words, in order for (8) to be convex, the objective
 158 function has to be concave, which is not the case, and does not incorporate this non-convex constraint.

159 A first alternative to solve the problem is via SDP relaxation, as described in (Luo et al., 2010), where the
 160 scalar products are replaced by the trace matrix operator

$$\begin{aligned}
 & \underset{\{\mathbf{W}_n\}}{\text{maximize}} && \text{Trace} \{\mathbf{R}_n \mathbf{W}_n\} \\
 & \text{subject to} && \text{Trace} \{\mathbf{R}_m \mathbf{W}_n\} \leq P_m, \text{ for } m \neq n \quad (\text{C0}) \\
 & && \text{Trace} \{\mathbf{W}_n\} \leq P_{\max}, \quad (\text{C1}) \\
 & && \mathbf{W}_n \geq 0, \quad (\text{C2})
 \end{aligned} \tag{9}$$

161 We note that in (9), the optimization variable is now a matrix, \mathbf{W}_n . In order for (9) to be equivalent to (8),
 162 (9) should incorporate the rank-1 constraint of \mathbf{W}_n (i.e., $\mathbf{W}_n = \mathbf{w}_n \mathbf{w}_n^H$). However, (9) relaxes (8). This is
 163 the so-called SDP relaxation. This relaxation is suboptimal, albeit the case of three or less constraints, as it
 164 is proved in (Luo et al., 2010; Beck and Eldar, 2006). We note that the complexity of the SDP relaxation is
 165 of $O(N^{4.5} \log(1/\epsilon))$, where $\epsilon > 0$ is the solution accuracy.

166 A second alternative that presents less complexity and can cope with any number of quadratic constraints
 167 can be designed if we take advantage of the fact that the correlation matrix of the desired user (\mathbf{R}_n) and
 168 of the interfered channels (\mathbf{R}_m), are rank-1 due to the Line-of-sight channel (LOS) in GEO satellites.
 169 Therefore, $\mathbf{w}_n^H \mathbf{R}_n \mathbf{w}_n = |\mathbf{h}_n^H \mathbf{w}_n|^2$, and both the objective function and the set of constraints in (8) are
 170 unchanged when an arbitrary phase rotation $\exp^{j\theta}$ is applied to \mathbf{w}_n . With that we can assume that $\mathbf{h}_n^H \mathbf{w}_n$ is
 171 a real number, i.e.,

$$\begin{aligned}
 & \text{Re} \left\{ \mathbf{h}_n^H \mathbf{w}_n \right\} \geq 0 \\
 & \text{Im} \left\{ \mathbf{h}_n^H \mathbf{w}_n \right\} = 0.
 \end{aligned} \tag{10}$$

172 By combining (10) and (8), the optimization problem can be converted to,

$$\begin{aligned}
 & \underset{\{\mathbf{w}_n\}}{\max} && \text{Re} \left\{ \mathbf{h}_n^H \mathbf{w}_n \right\} \\
 & \text{s.t.} && \text{Im} \left\{ \mathbf{h}_n^H \mathbf{w}_n \right\} = 0, \quad (\text{C0}) \\
 & && |\mathbf{h}_m^H \mathbf{w}_n|^2 \leq P_m, \text{ for } m \neq n \quad (\text{C1}) \\
 & && |\mathbf{w}_n|^2 \leq P_{\max}, \quad (\text{C2})
 \end{aligned} \tag{11}$$

173 The problem in (11) corresponds to a convex form known as SOCP (Boyd and Vandenberghe, 2004; Luo,
 174 2003), which can be solved via the interior point method. The solution to (11) will be henceforth referred
 175 as optimal solution.

176 A third alternative that offers an analytical solution is to relax (8) in order to transform it into the
 177 optimization of a Rayleigh quotient. The sub-optimal formulation is achieved by replacing (C1) and (C2)
 178 in (8) with a single tighter constraint. This can be done by exploiting the properties of the harmonic mean

(Lagunas et al., May 2020). In particular, (C1) and (C2) can be replaced by,

$$\left(\sum_{m \neq n}^N \frac{\mathbf{w}_n^H \mathbf{R}_m \mathbf{w}_n}{P_m} + \frac{\mathbf{w}_n^H \mathbf{w}_n}{P_{max}} \right)^{-1} \geq 1. \quad (12)$$

The resulting relaxed optimization problem is given by,

$$\begin{aligned} \max_{\{\mathbf{w}_n\}} \quad & \mathbf{w}_n^H \mathbf{R}_n \mathbf{w}_n \\ \text{s.t.} \quad & \mathbf{w}_n^H \left(\sum_{m \neq n}^N \frac{P_{max}}{P_m} \mathbf{R}_m + \mathbf{I} \right) \mathbf{w}_n = P_{max}, \end{aligned} \quad (13)$$

whose solution is given by the following generalized eigenvector form,

$$\mathbf{R}_n \mathbf{w}_n^* = \lambda_{max} \left(\sum_{m \neq n}^N \frac{P_{max}}{P_m} \mathbf{R}_m + \mathbf{I} \right) \mathbf{w}_n^*. \quad (14)$$

In particular, the solution to the relaxed problem (\mathbf{w}_n^*) is given by the eigenvector associated to the maximum eigenvalue of the matrix $\mathbf{R}_n^{-1} \left(\sum_{m \neq n}^N \frac{P_{max}}{P_m} \mathbf{R}_m + \mathbf{I} \right)$.

An advantage of the obtained precoder with respect to the optimal solution in (11) is fourfold: (1) A closed-form non-iterative solution can be obtained; (2) processing time to obtain the solution is in general reduced; (3) ability to cope with multipath propagation channels, and (4) can be applied when there are more receivers than number of beams.

In order to provide a connection with the RZF precoder design, let us assume that \mathbf{R}_n is rank-1, i.e. $\mathbf{R}_n = \mathbf{h}_n \mathbf{h}_n^H$. By substituting it into (14), the harmonic mean based solution only requires a matrix inversion,

$$\mathbf{w}_n \propto \left(\sum_{m \neq n}^N \frac{P_{max}}{P_m} \mathbf{R}_m + \mathbf{I} \right)^{-1} \mathbf{h}_n, \quad (15)$$

which presents the same complexity as in (7) (an upper bound complexity is $O(N^3)$, see (Golub and Loan, 1996)). Note that (12) is not exactly the harmonic mean because the factor $N - 1$ is not present. To finalize the design, the norm of the obtained precoder should be scaled in order to be equal to $\min \left(P_{max}, \frac{P_m}{\mathbf{w}_n^H \mathbf{R}_m \mathbf{w}_n} \right)$. Next, we study under which conditions the solution of this relaxed problem coincide with that of (11).

4.1 Relationship between the optimal and the relaxed solution

Assuming $\mathbf{R}_m = \mathbf{h}_m \mathbf{h}_m^H$ and applying the Karush–Kuhn–Tucker (KKT) conditions to (11) (Boyd and Vandenberghe, 2004), we can obtain the following solution to the convex problem,

$$\mathbf{w}_n \propto \left(\sum_{m \neq n}^N \lambda_m \mathbf{R}_m + \gamma \mathbf{I} \right)^{-1} \mathbf{h}_n, \quad (16)$$

where \mathbf{w}_n is the optimal precoder for the n -th beam, $\lambda_m, m = 1, \dots, N, m \neq n$ and γ are the Lagrangian variables of (C1) and (C2), respectively. In those scenarios when all the constraints are active with equality, $\lambda_m \neq 0, \gamma \neq 0$ (i.e., due to the KKT conditions), it is not possible to find a closed-form solution. However, whenever only one condition is active with equality, only the corresponding Lagrangian variable λ_m is different from zero and the problem presents an analytical solution. In order to illustrate this fact, let us assume that, due to the particular scenario settings, there is only one active constraint in (C1) and that (C2) is not fulfilled with equality (i.e., P_{max} is not the limiting constraint), then (16) simplifies to the minimum variance precoder for \mathbf{R}_n rank-1.

$$\mathbf{w}_n \propto (\mathbf{R}_n)^{-1} \mathbf{h}_n, \quad \text{for } m, n = 1, 2, n \neq m. \quad (17)$$

Alternatively, if only P_{max} is the limiting constraint, and therefore only (C2) is fulfilled with equality, then the matched precoder results

$$\mathbf{w}_n \propto \mathbf{h}_n. \quad (18)$$

Note that the solution (15) of the relaxed problem is also a particular case of (16), which appears when there is only one interference constraint (i.e., $P_m = P_1, m = 1$) and the scenario settings are such that $\frac{\gamma}{\lambda} = \frac{P_1}{P_{max}}$. Figures 2 illustrate this particular setting for a scenario with 2 beams, $P_1 = 5$ dBW, and the desired and unintended terminals are quite close to each other, as illustrated in Fig. 2(left). Fig. 2(middle) plots the optimal values of the two dual variables for different $\frac{P_1}{P_{max}}$ settings, with P_{max} ranging from 10 dBW to 30 dBW. The curve $\gamma = \lambda \frac{P_1}{P_{max}}$ is also plotted; as its crossings with the curve that corresponds to the optimal values of γ determine graphically those working points where the solution formulated in (16) is optimal. To better appreciate the crossing point, Fig. 2(right) provides a zoom on the relevant area. Fig. 3 shows the corresponding received power at each coverage point to verify that the optimal values of \mathbf{w}_n , when it is computed by solving (11) or, by the relaxed solution (14), are the same.

For the rest of the scenarios, having replaced the constraints by its harmonic mean provides a more conservative solution.

5 SIMULATION RESULTS

We now demonstrate the benefits of our proposed precoding scheme in a multibeam GEO satellite system. We consider a full frequency reuse broadband multibeam satellite that employs precoding to mitigate the resulting interbeam interference.

For the following numerical results, we consider a given satellite beam radiation pattern, whose complex coefficients at each user location, i.e. $[\mathbf{L}]_{n,i}$, have been provided by the European Space Agency (ESA) and correspond to a Direct Radiating Array (DRA) hypothetical pattern generated with internal software in the 20 GHz band, with 750 elements spaced 5λ (with λ denoting the wavelength). Satellite position is 13°E . For the purposes of the present work, only a subset of $N = 7$ beams will be considered for the precoding design, as illustrated in Fig. 4. For the scenario at hand, we assume perfect CSI available at the satellite gateway.

In addition, we consider $G_R = 39.75$ dBi, carrier frequency of 20 GHz, user bandwidth of $B = 500$ MHz, a dish noise temperature of $T = 50^\circ\text{K}$, a noise figure of 2.278 dB and the true slant range distance for d_n . Regarding the satellite transmitted power, we assume a maximum of $P_{max} = 20$ dBW per beam (including additional payload losses η).

First of all, we evaluate the condition number of the matrix $(\mathbf{H}\mathbf{H}^H)$, which motivates the use of RZF precoding and the proposed technique. In Fig. 5, we show the average SINR obtained when applying ZF precoding (6), RZF precoding (7), and both the proposed optimal scheme (11) and the proposed sub-optimal one in (14) (based on the harmonic mean relaxation), versus the condition number of the matrix $(\mathbf{H}\mathbf{H}^H)$ (which varies depending on the scheduled users at each realization). We solve the proposed precoding technique in (11) with standard optimization software, e.g. (Grant and Boyd, 2014). We set the tolerable interference level based on $P_m/\sigma_n^2 = -10\text{dB}$, which corresponds to $P_m = -128\text{ dBW}$. In Fig. 5, we observe that both ZF and RZF precoding experience significant performance loss as the condition number increases, being the latter more pronounced for ZF precoding. On the other hand, both the proposed techniques, i.e. the optimal one (11) and the so-called harmonic mean (14) tend to provide the same average SINR which is in general higher than that of the conventional schemes.

One of the advantages of the proposed technique is that it allows to work with more users than the number of available degrees of freedom (i.e., beams). To show this, we consider the $N = 7$ beam scenario, where the precoder is designed to transmit simultaneously to more users than beams. Fig. 6 shows the resulting SINR for a desired user located in beam 4 of Fig. 4, which receives interference from the rest of the cochannel beams $M \geq N - 1$ users (i.e., the so-called unintended users). These unintended users are randomly distributed within the coverage area of the 7 beams. Fig. 6 shows the performance of the optimal precoding design (11) and the relaxed solution (14) for different values of M , and compares with two benchmark schemes that are detailed in the following. Due to the good performance of (14), which is based on the harmonic mean relaxation, we have included in Fig. 6 the relaxation of the problem considering the arithmetic mean. In particular, the arithmetic mean relaxation reduces (11) by substituting all the constraints in (C1) by just their arithmetic mean (i.e., $\sum_{m \neq n}^N \frac{1}{N-1} \mathbf{R}_m \leq P_m$). The second benchmark depicted in Fig. 6 is the RZF precoding design of (7) (proposed in (Peel et al., 2005)). From Fig. 6 it can be observed that the SINR of the desired user decreases as the number of unintended user increases. More importantly, the performance of the proposed harmonic mean based relaxation, which is more conservative than the arithmetic mean and the optimal approach, is shown to outperform the benchmark schemes by providing significantly higher SINR.

Going back to the scenario of one scheduled user per beam, let us focus on a particular instance, where the scheduled users render a high condition number of $(\mathbf{H}\mathbf{H}^H)$, i.e. 352, $P_{max} = 20\text{ dBW}$, $P_m = -128\text{ dBW}$. The detailed user locations are depicted in Fig. 7, where we can observe that beam 5 and beam 7 have scheduled users that are very close to each other. If we apply conventional RZF to this particular instance, we obtain the SINR shown in blue in Fig. 8. Clearly, the singularity of matrix $(\mathbf{H}\mathbf{H}^H)$, and in particular the similarity of the channel vectors \mathbf{h}_5 and \mathbf{h}_7 , has impact on the RZF precoding performance for the affected beams. In other words, the RZF has to devote more power than the other techniques in Fig. 8 to null out the strong cochannel interference, thus reducing the gain towards the desired user. Furthermore, Fig. 8 shows the SINR values achieved with both the proposed precoding techniques (11) and (14) in green and yellow, respectively, assuming $P_{max} = 20\text{ dBW}$, $P_m = -128\text{ dBW}$, and it can be clearly observed that relaxing the tolerable interference levels has a positive impact on the overall SINR.

To understand better the details of the scheduling instance shown in Fig. 7, Fig. 9 shows the received power at the intended user for each beam in the upper part of the figure, while the bottom part shows the received power at the worst co-channel user for each beam. The worst cochannel user is the one who receives the highest interference level from each of the listed beams. First of all, it can be observed that the received power at the worst cochannel users for both the proposed techniques is always below $P_m = -128\text{ dBW}$. Focusing on the received power at the cochannel users, the RZF scheme is clearly suffering with the

matrix inversion and the regularized factor is not able to counteract the effect caused by two scheduled users closely located. While relaxing the interference constraints to the cochannel beams, the proposed schemes are able to steer more power into the desired users. This can be seen in the upper part of Fig. 9, where a significant improvement in the received useful power is achieved with the proposed precoding with received-interference power constraints.

Finally, we run a total of 500 Monte Carlo realizations by randomly placing the user terminals. The distribution of the resulting matrix condition number of $(\mathbf{H}\mathbf{H}^H)$ is depicted in Fig. 10, where it can be seen that there are large number of cases where the selected users render a challenging precoding scenario due to their channel similarities. The effect of the selected scheduled users on the final achievable capacity is depicted in Fig. 11 in terms of Cumulative Distribution Function (CDF). We compare the sum rate of both the optimal and the relaxed harmonic mean scheme ($P_{max} = 20$ dBW, $P_m = -128$ dBW) with the ZF and RZF benchmarks (i.e., the sum rate is computed from (5) as $\sum_n^N r_n$). It can be observed that the proposed schemes outperform the benchmarks in most of the cases. This means that scheduling is not so critical, thus alleviating one of the most challenging design issue of precoding implementation, while achieving significant gains via the proposed precoding scheme. To better appreciate the difference between the optimal proposed solution and the relaxed one, Fig. 12 shows a zoom of the CDF depicted in Fig. 11. As expected, the relaxed solution attains a slightly lower rate due to the received-interference lower bound resulting from the harmonic mean of all the interference constraints.

6 CONCLUSIONS

In this paper, we have proposed a new precoding design framework which imposes received-interference power constraints at the cochannel users, in an attempt to relax the design of conventional schemes that rely on the channel matrix inversion. By allowing some residual received interference, we show that the proposed design is able to provide significant gains when unlucky scheduling events occur (i.e. those rendering an ill-conditioned channel matrix). We also study in detail the effects of relaxing the optimization by substituting the interference constraints with an harmonic based mean. We validate and compare the proposed designs through extensive numerical simulation experiments, showing better results in terms of SINR and rate. The proposed designs are also more robust to user scheduling, and the presented harmonic mean relaxation stands out as the most promising solution in terms of performance and computational complexity. Regarding the impact of imperfect CSI, we do not expect a strong impact related to outdated CSI because the coherence period of the channel between GEO satellite and fix terminal users is generally long. However, we expect the errors on the estimation process to have an impact, particularly in the feasibility of the interference constraints. An alternative to prevent such cases is to add a conservative margin to the interference constraints (e.g. proportional to the estimation error magnitude).

CONFLICT OF INTEREST STATEMENT

The authors declare that the research was conducted in the absence of any commercial or financial relationships that could be construed as a potential conflict of interest.

AUTHOR CONTRIBUTIONS

E. Lagunas and A. Pérez-Neira led the main contribution and writing of the manuscript. E. Lagunas, A. Pérez-Neira and M. Martínez carried out the experimental evaluation. M.A. Lagunas conceived the original idea and provided supervision. M.A. Vázquez contributed to the developed techniques. B. Ottersten supervised the findings of this work. All authors contributed to the manuscript and approved the submitted version.

FUNDING

318 This work has been partially supported by the Luxembourg National Research Fund (FNR) under the
 319 project FlexSAT (C19/IS/13696663) and by the ministry of Science, Innovation and Universities, Spain,
 320 under project TERESA -TEC2017-90093-C3-1-R (AEI/FEDER, UE).

REFERENCES

- 321 Arapoglou, P.-D., Ginesi, A., Cioni, S., Erl, S., Clazzer, F., Andrenacci, S., et al. (2016). Dvb-s2x-enabled
 322 precoding for high throughput satellite systems. *International Journal of Satellite Communications and*
 323 *Networking* 34, 439–455. doi:10.1002/sat.1122
- 324 Bandi, A., Shankar M. R, B., Chatzinotas, S., and Ottersten, B. (2020). A joint solution for scheduling and
 325 precoding in multiuser miso downlink channels. *IEEE Transactions on Wireless Communications* 19,
 326 475–490. doi:10.1109/TWC.2019.2946161
- 327 Beck, A. and Eldar, Y. (2006). Strong duality in nonconvex quadratic optimization with two quadratic
 328 constraints. *Journal of the Society for Industrial and Applied Mathematics, SIAM J. OPTIM.*, 17,
 329 844–860
- 330 Bengtsson, M. and Ottersten, B. (1999). Optimal Downlink Beamforming Using Semidefinite Optimization.
 331 *Annual Allerton Conference on Communication, Control, and Computing*, 987–996
- 332 Bengtsson, M. and Ottersten, B. (2001). *Book Chapter: Optimal and Suboptimal Transmit Beamforming*
 333 (CRC Press), chap. in *Handbook of Antennas in Wireless Communications* edited by L.C. Godara
- 334 Bjornson, E., Bengtsson, M., and Ottersten, B. (Jul. 2014). Optimal Multiuser Transmit Beamforming: A
 335 Difficult Problem with a Simple Solution Structure [Lecture Notes]. *IEEE Signal Processing Magazine*
 336 31, 142–148
- 337 Boyd, S. and Vandenberghe, L. (2004). *Convex Optimization* (Cambridge University Press)
- 338 Cailloce, Y., Caille, G., Albert, I., and Lopez, J. (2000). A ka-band direct radiating array providing multiple
 339 beams for a satellite multimedia mission. In *Proceedings 2000 IEEE International Conference on*
 340 *Phased Array Systems and Technology (Cat. No.00TH8510)*. 403–406. doi:10.1109/PAST.2000.858984
- 341 Christopoulos, D., Chatzinotas, S., and Ottersten, B. (2015). Multicast multigroup precoding and user
 342 scheduling for frame-based satellite communications. *IEEE Transactions on Wireless Communications*
 343 14, 4695–4707. doi:10.1109/TWC.2015.2424961
- 344 Devillers, B., Perez-Neira, A., and Mosquera, C. (2011). Joint linear precoding and beamforming for the
 345 forward link of multi-beam broadband satellite systems. In *2011 IEEE Global Telecommunications*
 346 *Conference - GLOBECOM 2011*. 1–6. doi:10.1109/GLOCOM.2011.6133895
- 347 ESA project LiveSatPreDem (2020). Live Satellite Precoding Demonstration [https://artes.esa.](https://artes.esa.int/projects/livesatpredem)
 348 [int/projects/livesatpredem](https://artes.esa.int/projects/livesatpredem)
- 349 Gershman, A. B., Sidiropoulos, N. D., Shahbazpanahi, S., Bengtsson, M., and Ottersten, B. (2010). Convex
 350 optimization-based beamforming. *IEEE Signal Processing Magazine* 27, 62–75. doi:10.1109/MSP.2010.
 351 936015
- 352 Golub, G. H. and Loan, C. F. V. (1996). *Matrix Computations* (John Hopkins University Press)
- 353 Grant, M. and Boyd, S. (2014). CVX: Matlab software for disciplined convex programming, version 2.1
 354 <http://cvxr.com/cvx>
- 355 Guidotti, A. and Vanelli-Coralli, A. (2018). Geographical scheduling for multicast precoding in multi-beam
 356 satellite systems. In *2018 9th Advanced Satellite Multimedia Systems Conference and the 15th Signal*
 357 *Processing for Space Communications Workshop (ASMS/SPSC)*. 1–8. doi:10.1109/ASMS-SPSC.2018.
 358 8510728

- Joroughi, V., Vazquez, M., and Perez-Neira, A. (Feb. 2017). Cross-layer packet scheduler design of a multibeam broadband satellite system with adaptive coding and modulation. *IEEE Trans. Wireless Communications* 16, 952–966
- Kodheli, O. et al. (2020). Satellite Communications in the New Space Era: A Survey and Future Challenges. *IEEE Communications Surveys Tutorials* ArXiv:2002.08811
- Lagunas, E., Andrenacci, S., Chatzinotas, S., and Ottersten, B. (2018). Cross-layer forward packet scheduling for emerging precoded broadband multibeam satellite system. In *2018 9th Advanced Satellite Multimedia Systems Conference and the 15th Signal Processing for Space Communications Workshop (ASMS/SPSC)*. 1–8. doi:10.1109/ASMS-SPSC.2018.8510717
- Lagunas, E., Pérez-Neira, A., Lagunas, M., and Vázquez, M. (May 2020). Transmit Beamforming Design with Received-Interference Power Constraints: The Zero-Forcing Relaxation. *IEEE Int. Conf. on Acoustics, Speech, and Signal Processing (ICASSP), Barcelona, Spain*
- Luo, Z. (2003). Applications of convex optimization in signal processing and digital communication. *SPRINGER Mathematical Programming* 97, 177–207
- Luo, Z., Ma, W., So, A. M., Ye, Y., and Zhang, S. (2010). Semidefinite relaxation of quadratic optimization problems. *IEEE Signal Processing Magazine* 27, 20–34
- Peel, C. B., Hochwald, B. M., and Swindlehurst, A. L. (2005). A vector-perturbation technique for near-capacity multiantenna multiuser communication-part i: channel inversion and regularization. *IEEE Transactions on Communications* 53, 195–202. doi:10.1109/TCOMM.2004.840638
- Perez-Neira, A. I., Vazquez, M. A., Shankar, M. R. B., Maleki, S., and Chatzinotas, S. (2019). Signal processing for high-throughput satellites: Challenges in new interference-limited scenarios. *IEEE Signal Processing Magazine* 36, 112–131
- Taesang Yoo and Goldsmith, A. (2006). On the optimality of multiantenna broadcast scheduling using zero-forcing beamforming. *IEEE Journal on Selected Areas in Communications* 24, 528–541. doi:10.1109/JSAC.2005.862421
- Taricco, G. (2014). Linear precoding methods for multi-beam broadband satellite systems. In *European Wireless 2014; 20th European Wireless Conference*. 1–6
- Toso, G., Angeletti, P., and Mangenot, C. (2014). Multibeam antennas based on phased arrays: An overview on recent esa developments. In *The 8th European Conference on Antennas and Propagation (EuCAP 2014)*. 178–181. doi:10.1109/EuCAP.2014.6901721
- Vazquez, M. A., Perez-Neira, A., Christopoulos, D., Chatzinotas, S., Ottersten, B., Arapoglou, P., et al. (2016). Precoding in multibeam satellite communications: Present and future challenges. *IEEE Wireless Communications* 23, 88–95. doi:10.1109/MWC.2016.1500047WC
- Vorobyov, S. A., Gershman, A. B., and Zhi-Quan Luo (2003). Robust adaptive beamforming using worst-case performance optimization: a solution to the signal mismatch problem. *IEEE Transactions on Signal Processing* 51, 313–324. doi:10.1109/TSP.2002.806865
- Vázquez, M. ., Shankar, M. R. B., Kourogiorgas, C. I., Arapoglou, P., Icolari, V., Chatzinotas, S., et al. (2018). Precoding, scheduling, and link adaptation in mobile interactive multibeam satellite systems. *IEEE Journal on Selected Areas in Communications* 36, 971–980. doi:10.1109/JSAC.2018.2832778
- Zetterberg, P. and Ottersten, B. (1995). The spectrum efficiency of a base station antenna array system for spatially selective transmission. *IEEE Transactions on Vehicular Technology* 44, 651–660
- Zheng, G., Chatzinotas, S., and Ottersten, B. (2012). Generic optimization of linear precoding in multibeam satellite systems. *IEEE Transactions on Wireless Communications* 11, 2308–2320. doi:10.1109/TWC.2012.040412.111629

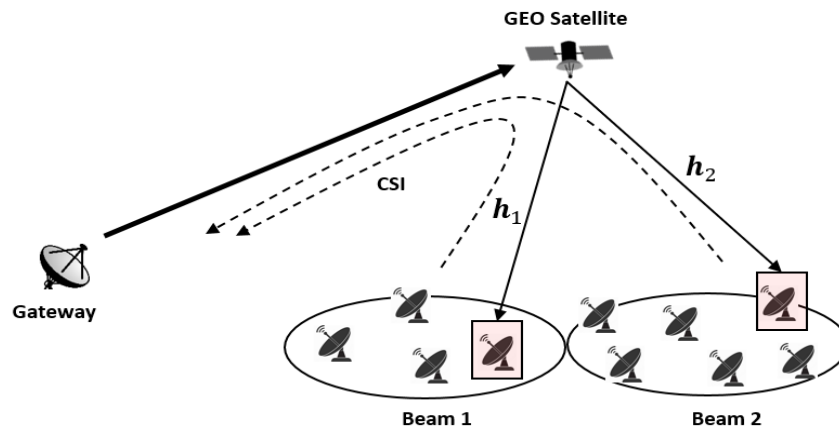


Figure 1. Simplified scheme of a 2-beam GEO system

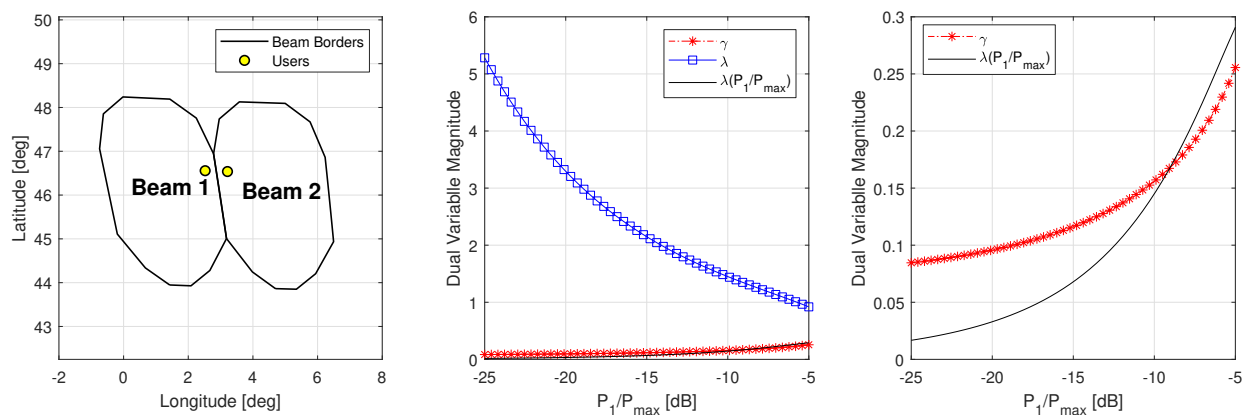


Figure 2. Dual Variables Evaluation: (left) Simplified scenario with 2 beams and 2 users (beam 1 contains the desired user; and beam 2 contains the unintended user); (middle) Optimal values of the dual variables when solving (16), $P_1 = 5$ dBW; and (right) Zoom on middle figure.

FIGURE CAPTIONS

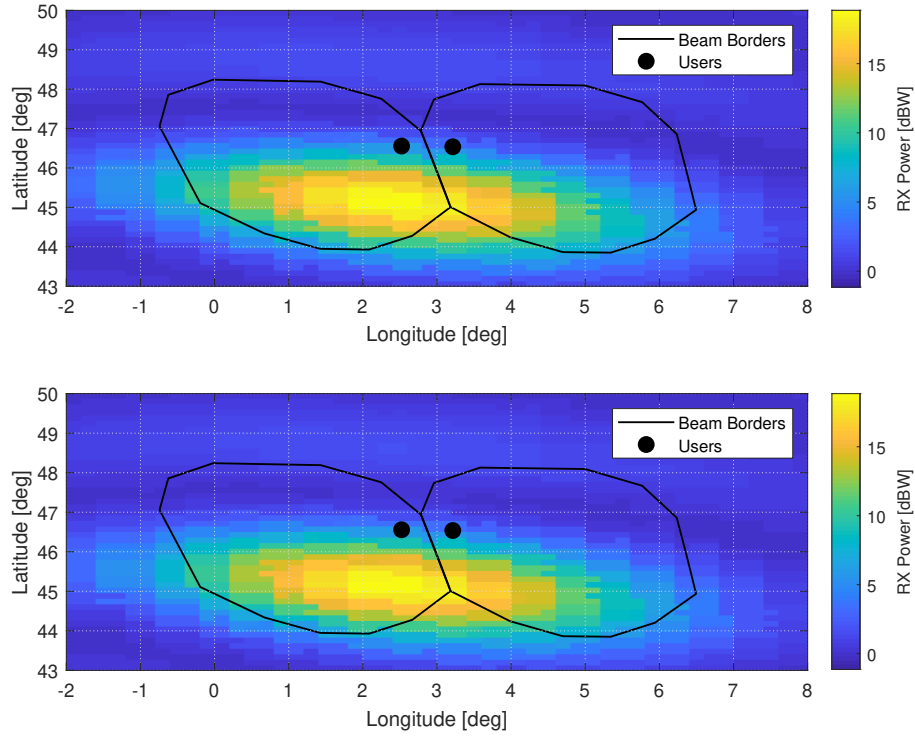


Figure 3. (top) Optimal beam pattern, desired user SINR = 3.1 dB; (bottom) Beam pattern obtained with the harmonic-mean constraint relaxation, desired user SINR = 3.1 dB

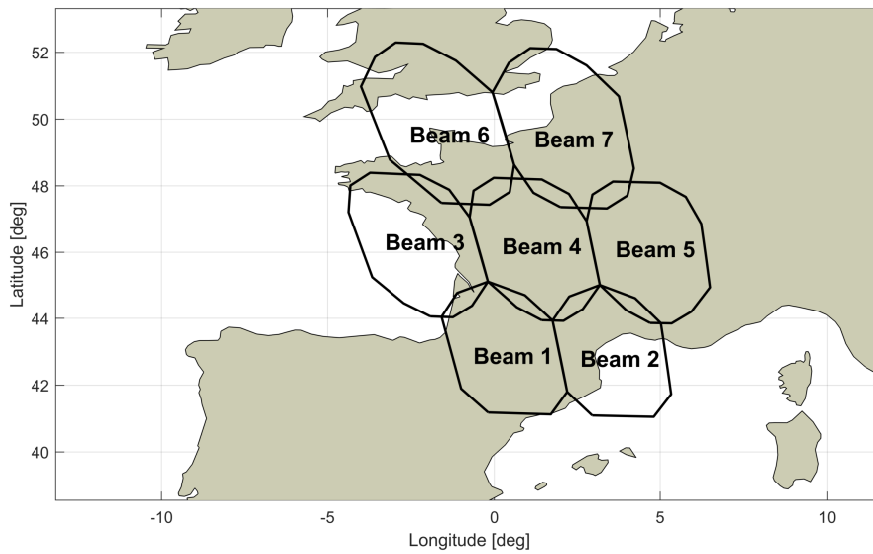


Figure 4. Cluster of $N = 7$ beams considered herein.

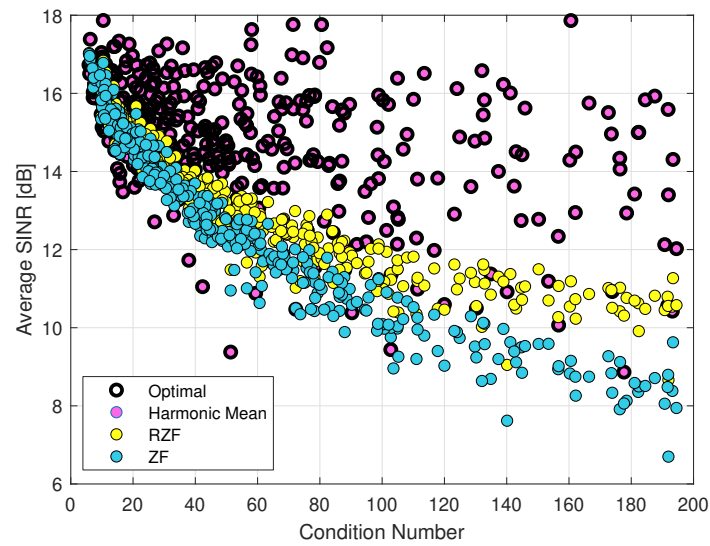


Figure 5. Average SINR [dB] versus Condition Number of the matrix ($\mathbf{H}\mathbf{H}^H$).

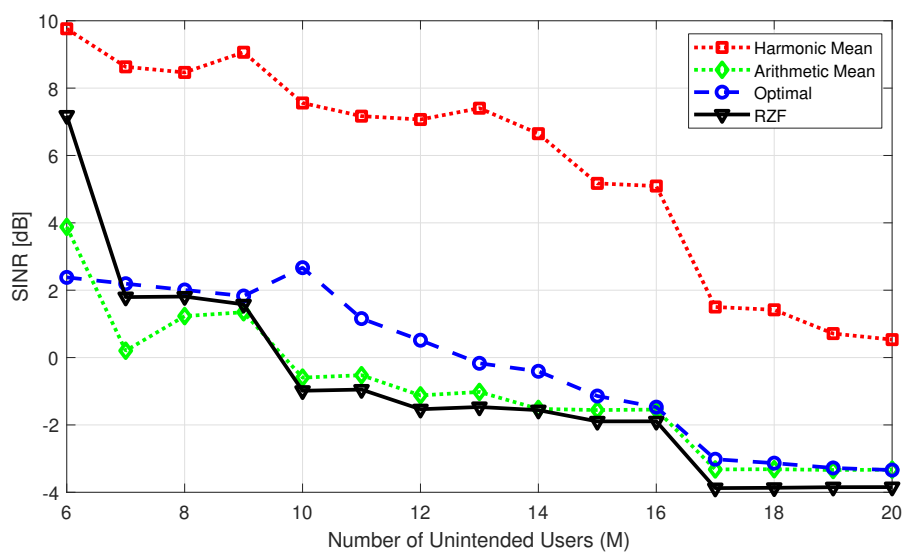


Figure 6. Achievable SINR when the number of unintended users is higher than the number of beams ($M \geq N-1$), $P_{max} = 15$ dBW, $P_m = 4$ dBW, $\forall m$.

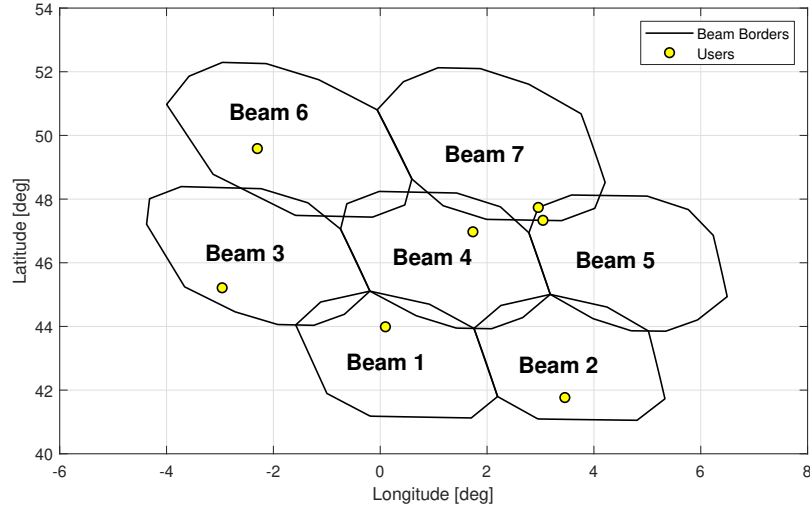


Figure 7. Considered user scheduling instance.

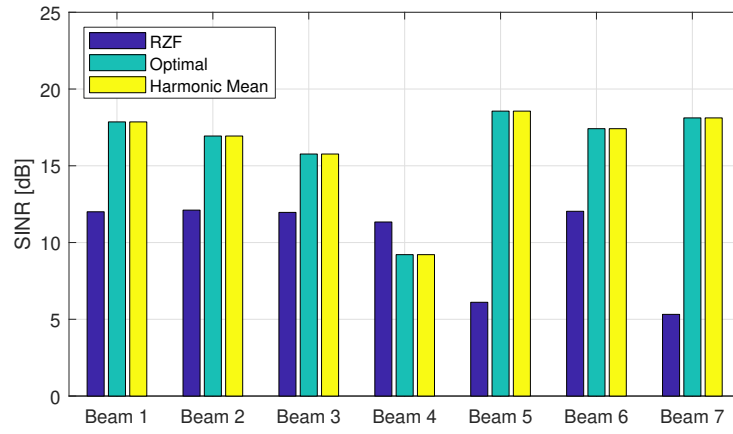


Figure 8. SINR per beam obtained with RZF and the proposed scheme, $P_{max} = 20$ dBW, $P_m = -128$ dBW

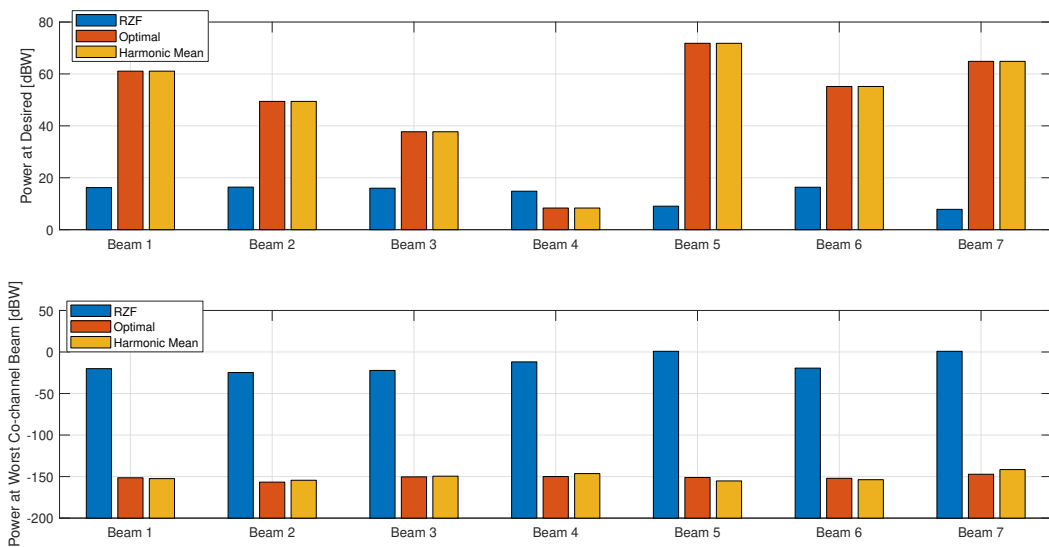


Figure 9. (up) Received power at the desired user; (bottom) Received power at the worst co-channel user. $P_{max} = 20$ dBW, $P_m = -128$ dBW

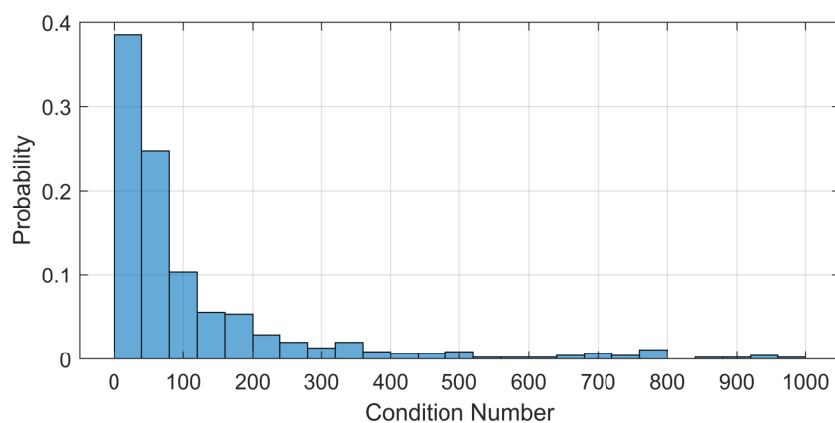


Figure 10. Histogram of Condition Number.

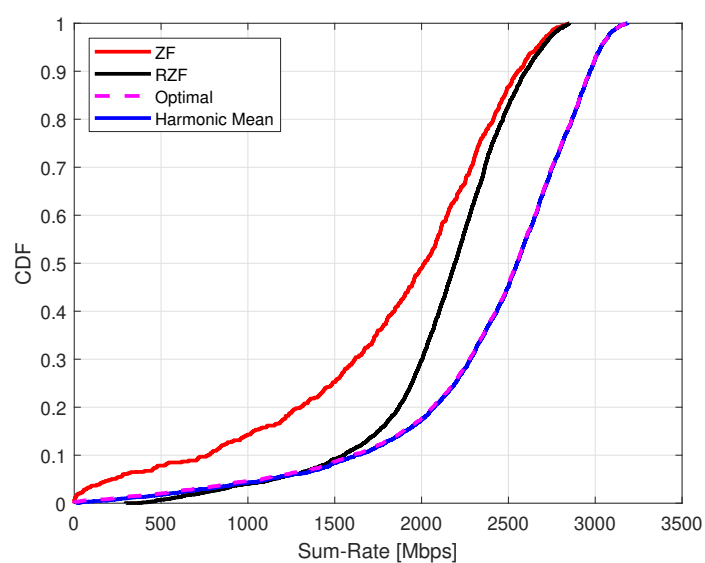


Figure 11. CDF of capacity distribution.

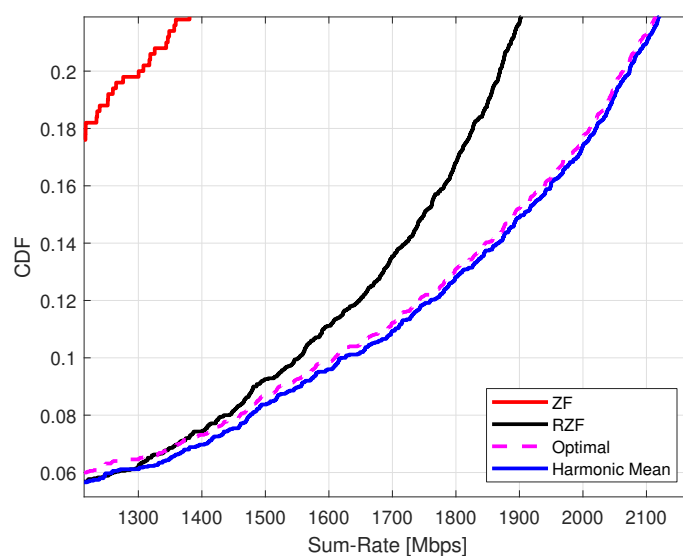


Figure 12. Zoom of Figure 11